



**SPECTROSCOPIC STUDIES OF IRON-BASED SCR
CATALYSTS – INVESTIGATION OF THERMAL
DEACTIVATION PROCESSES**

Emma Catherine Adams

07985452

Project Supervisors:

Professor J.A. Anderson

Professor M. Skoglundh

Soran Shwan, PhD.

Summary

The thermal stability of iron/beta (Fe/BEA) as an SCR catalyst was studied. Samples were treated in the absence of water at 700, 800 and 900°C for 6 to 48 hours and characterized by nitrogen physisorption and UV-vis spectroscopy. DRIFT spectroscopy was also used, not only to characterize the Fe species present, but also to correlate any changes in activity with changes in iron and/or zeolite structure.

Deconvolution of the UV-vis spectra showed an increase in the production of small clusters and larger surface particles with ageing time and temperature, with a subsequent reduction of isolated Fe²⁺ and Fe³⁺ ions. These results were in correlation with the NO temperature programmed desorption results of the DRIFTS experiments.

Ageing for extended periods of time and/or temperature resulted in a decrease in surface area of the zeolite and eventually zeolite collapse. This could be correlated to the reduction in Brønsted acid sites as found by the NH₃ temperature programmed desorption results of the DRIFTS experiments and is responsible for the reduction in ammonia adsorption capacity with ageing.

Declaration

This report is entirely my own composition. It has not been accepted in any previous application for a degree. It is a record of my work and all verbatim extracts have been distinguished by quotation marks. My sources of information have been specifically acknowledged.

Acknowledgements

I wish to thank my supervisors at Chalmers University of Technology, Soran Shwan and Professor Magnus Skoglundh, for their invaluable guidance and enthusiasm throughout this placement and everyone at the KCK department for being so welcoming and making my placement so enjoyable!

I would also like to thank my main supervisor, Professor Jim Anderson, for all the support he has given me over the year including securing this project and helping me with any problems I encountered along the way.

And most importantly, many thanks to my fantastic family for all their encouragement, love and support throughout my entire time at University.

Contents

1. Introduction	6
2. Experimental	
2.1. Catalyst preparation	12
2.2. UV-vis spectroscopy	12
2.3. BET characterization	12
2.4. In-situ DRIFTS studies	
2.4.1. <i>NH₃ TPD</i>	13
2.4.2. <i>NO TPD</i>	13
2.4.3. <i>SCR reaction</i>	13
3. Results and Discussion	
3.1. UV-vis analysis	14
3.2. BET characterization	16
3.3. DRIFTS spectroscopy	
3.3.1. <i>NH₃ TPD</i>	17
3.3.2. <i>NO TPD</i>	21
3.3.3. <i>SCR reaction</i>	23
4. Conclusions	26
5. References	27
Appendix a	30
Appendix b	31

1. Introduction

Although there are many sources for the generation of pollutants in the atmosphere, one of the main areas which can be controlled is the transport sector, hence regulations regarding emissions are becoming increasingly stringent^{1,2}. This regulation is necessary since there is an ever increasing demand for the energy required to power these vehicles, predominantly provided by the combustion of fossil fuels. This is a problem since it is known that the combustion process results in the formation of many harmful pollutants including nitrous oxides (NO_x , where $x=1$ or 2)³. The presence of NO_x in the atmosphere is responsible for various environmental issues including photochemical smog and acid rain which consequently results in the acidification of soils and water, impacting both plant and animal life^{4,5}. Currently the Euro 6 emission standards state that by September 2014, new light duty diesel vehicles should be producing a maximum of 0.08 g/km of NO_x whilst maintaining particulate matter and CO emissions at 0.05 and 0.5 g/km respectively⁶.

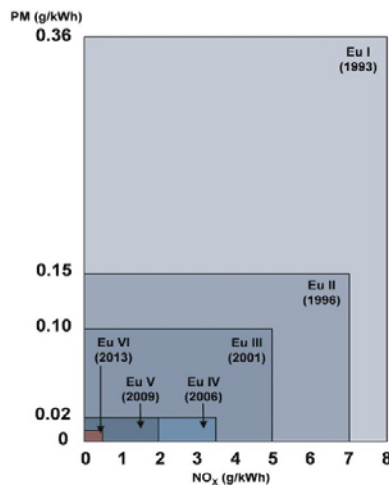
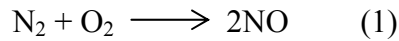


Figure 1: Comparison of Euro I-VI emission regulations for NO_x and particulate matter⁶

Diesel engines offer many environmental benefits over gasoline engines including lower CO_2 production due to better fuel efficiency^{7,8}. However, the main disadvantage of these systems is that they operate at high air-to-fuel ratios resulting in excess oxygen which subsequently causes difficulty in the ability to reduce the nitrous oxides which are formed in the exhaust gases^{2,5,9}.

The production of nitrous oxides is largely due to the occurrence of a free radical process in the high temperatures of the diesel engine, known as the Zeldovich mechanism, during which atmospheric nitrogen reacts with oxygen. This is known as thermal NO_x¹⁰;



It is estimated that diesel vehicles are responsible for about 75% of NO_x production in the automotive industry³. Thus it is of major importance to successfully develop a system capable of carrying out the reverse of reaction (1) to enable significant conversion of the pollutant back to pure N₂ and O₂ which are naturally present within the atmosphere and cause no threat to the environment. The difficulty in producing techniques capable of this is that the reaction, although thermodynamically possible, is limited by kinetics since the activation energy of this reaction is very high (364 kJ/mol)¹¹ and they must be active within the varying temperature conditions of the vehicle.

Catalysts are preferable for the abatement of NO_x since they can be implemented at low cost and show high efficiency¹². However, although it is inevitable that catalysts will eventually decay, their deactivation can prove costly if they need to be replaced frequently. The Euro 6 guidelines specify that the durability of the catalyst before testing for deterioration is necessary should be 100,000 km or 5 years, whichever comes first¹³.

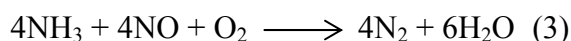
Although the conventional three way catalyst has been used to simultaneously remove NO_x, CO and HC successfully in the past, this technique requires stoichiometric air-to-fuel conditions and is no longer effective in reducing NO_x in the presence of elevated oxygen^{1,14}. Therefore, there is a need to produce more efficient techniques suitable for NO_x abatement in lean conditions.

At present, there has been little success in finding suitable catalysts which have the potential to carry out the conversion of NO_x in significant volume whilst subjected to the conditions which are commonly found in vehicles although selective catalytic reduction (SCR) catalysts represent one of the most effective strategies for reducing NO_x^{15,16,17}. During this process, a reducing agent (in the form of ammonia or hydrocarbons) is required in order to selectively react with the nitrogen oxides and not with the excess oxygen present¹⁸. For the purposes of this investigation, ammonia will be the reducing agent focused upon as it has been implemented for use by many companies such as Volvo, Iveco and Renault in heavy duty vehicles⁸. As there are problems with the storage of pure ammonia due to its toxicity, it must

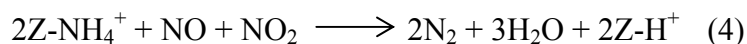
be supplied to the exhaust pipe by the injection of urea (NH₂-CO-NH₂), which is stored in a separate tank¹⁹. Once injected it is subject to hydrothermal conditions and subsequently becomes hydrolysed in order to produce a source of ammonia^{20,21};



Once this conversion has taken place and ammonia is available in the exhaust gases, it is possible to carry out the reaction known as the “standard-SCR”^{22,16};



However, in practice it is necessary for a fraction of this NO to be oxidized to adsorbed NO₂ species thus limiting the rate of the SCR reaction²². It is also accepted that the Brønsted acidity of the catalyst plays a role in its activity as it is necessary for both the binding and activation of ammonia species^{23,3}. Once ammonium ions are present on the catalyst surface, they are able to react with nearby gaseous or weakly adsorbed NO_x species to form nitrogen and water. This mechanism is consistent with an Eley-Rideal type mechanism as proposed by many groups and implies that the catalyst support itself has a significant effect on SCR activity²³;



(where Z = zeolite)

Although vanadia based catalysts have been implemented for use as SCR catalysts in both stationary and mobile applications for many years, they are not ideal for use in transport as they become rapidly deactivated by strong surface adsorption of sulphur^{24,9}. This poisoning is a major disadvantage since sulphur species (SO₂ and SO₃) are commonly found in both engine oils and fuel. It is therefore of importance to investigate materials which do not exhibit this intolerance to the presence of such species. There are also problems with the narrow temperature range in which they operate since a rapid decrease in activity and selectivity is observed at temperatures above 550°C and there is further concern regarding toxicity above 650°C due to the volatilization of the material^{10,3}. Therefore, not only is resistance to poisoning important in the production of suitable catalysts, but thermal stability is also of paramount interest.

Metal-exchanged zeolites have been extensively reported as suitably active materials for the conversion of NO_x species to nitrogen and water in some cases showing 100% NO conversion

within the temperature range 450 to 500°C²⁴. Most importantly, their performance remains unaffected when in the presence of both sulphur and water at low temperature²⁴. Beta (BEA) zeolite is a particularly promising catalyst for the reduction of NO_x because it is composed of a network of large 12-membered ring micropores which allows, not only for fast and easy diffusion of reactants and products throughout the structure²⁵, but their large surface area also leads to an increased ammonia adsorption capacity²⁶. However, the pores should not be too large or the activity of the catalyst will be hindered since the Brønsted acid sites must be close enough to allow the reaction between the adsorbed ammonium and NO_x species as previously discussed.

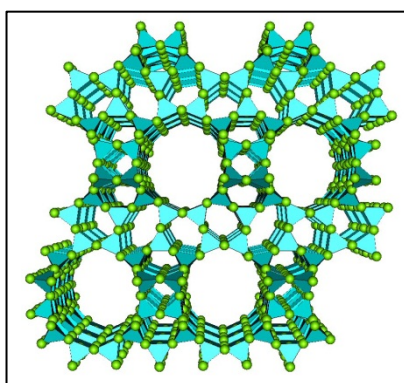


Figure 2: Structure of BEA zeolite framework²⁷

Iron-exchanged zeolites in particular have been shown to have not only high activity and selectivity for the urea-SCR reactions but also have greater thermal stability than their vanadium counterparts^{28,26}. They are able to operate over a wide temperature range which is important because of the variation in temperature experienced within diesel exhaust systems as a result of different driving conditions such as cold starts, inactive periods, fast driving and heavy loads. There are, however, problems with the hydrothermal stability of these materials above 500°C²⁹ and since the regeneration of the diesel particulate filter has been reported to occur at temperatures between 600 to 800°C with the production of steam, degradation of the zeolite and therefore loss of performance is inevitable³⁰.

Due to the crystalline structure of the zeolite, well-defined structures with known position and environment are formed when transition metals are impregnated into their network³¹. It is well known that iron species can coexist in the zeolite network in various forms; isolated and binuclear iron ions at ion exchange positions, small oligonuclear Fe_xO_y clusters in the micropores and large agglomerates of Fe₂O₃ on the external surface^{25,32,33,34}. However, there

is much debate over the role which each of these species plays in the overall SCR reaction, with many different active sites being postulated^{35,36}. Understanding these roles at a molecular level, and therefore the mechanisms of urea-SCR on transition metal zeolites, would aid in the development of improved catalysts which are more stable and suitable for use at high temperature³⁷.

The two main deactivation mechanisms which have been proposed by several groups regarding the thermal stability of metal exchanged zeolites include;

1. A loss of support area due to zeolite collapse and therefore dealumination of Brønsted acid sites^{38,30}. Rahkamaa-Tolonen *et al*¹ found that the reduction in Brønsted acidity of the catalyst during hydrothermal aging was caused by the dealumination of the zeolite structure. This takes place when Al³⁺ ions which form part of the tetrahedral network migrates out of the structure as a result of the instability of the Si-O-Al bonds compared to Si-O-Si bonds with regards to their vulnerability to water attack. This process has a direct impact upon the reduction of NO_x as Long *et al*³⁹ determined that the Brønsted sites on zeolites act as active sites for ammonia adsorption. As temperature increases further, the catalyst begins to decay. This process also often leads to plugging of the pores within the zeolite structure due to accumulation of the alumina⁴⁰.
2. A migration of iron ions which results in the formation of large metal-oxide clusters considered to have reduced activity²⁹. However, as yet there have been no conclusions regarding the specific activity of these larger iron species under SCR conditions as it is difficult to isolate them.

However, these are mechanisms which have been postulated to take place in the presence of water and minimal work has been conducted in the absence of water. It would therefore be of interest to investigate the effect, if any, which temperature alone has on Fe/BEA in order to gain a better understanding of the mechanisms taking place in the SCR reactions.

One of the most commonly utilized techniques for the in-situ characterization of adsorption/desorption of gaseous species on solid surfaces in catalysis is diffuse reflectance infrared transform spectroscopy (DRIFTS). It is an advantageous technique since it allows for the ability to simultaneously obtain information on both the reaction mechanisms and the structure of the catalyst. It also allows for the control of temperature and environment within the cell and no requirement for pretreatments on the sample such as dilution⁴¹. The intensity of the infrared band formed upon absorption of a photon is proportional to the change in

dipole moment of the functional group. Therefore, observed frequency bands are characteristic of specific bonds within the molecules and can be used to identify species adsorbed on the surface. This technique, although highly sensitive, does not give quantitative information about the characteristics of the samples and this must be kept in mind when analyzing spectra. The bulk of this report will therefore focus upon this method to follow the effects of ageing upon the SCR reaction of the catalysts.

The aim of the present project is to investigate the deactivation of urea-SCR catalyst Fe/BEA zeolite as a result of thermal ageing in the absence of water in order to suggest possible mechanisms behind the reduced activity. This investigation has been done in parallel with the project carried out by Soran Shwan, PhD at the Competence Centre for Catalysis, Göteborg on the hydrothermal ageing of Fe/BEA.

2. Experimental

2.1. *Catalyst preparation*

The 1.0 wt. % Fe/BEA zeolite catalyst was prepared by the incipient wetness impregnation method. An aqueous solution of $\text{Fe}(\text{NO}_3)_3 \cdot 9\text{H}_2\text{O}$ was used for impregnation of Fe into BEA zeolite powder (Zeolyst International). The prepared catalyst was oven dried at 120°C overnight followed by calcination in air by slowly heating to 450°C ($2^\circ\text{C}/\text{min}$) and preserved at this temperature for 3 hours.

In order to thermally age the samples, the produced catalyst was then split into four lots and heated in an oven in the absence of water to 700°C ($5^\circ\text{C}/\text{min}$) and maintained at this temperature for either 6, 12, 24 or 48 hours. A fifth lot was left un-aged so that a direct comparison could be made between the fresh and aged catalysts. This ageing process was then repeated at 800°C and 900°C for 48 hours only to investigate the effect of temperature on the activity of the prepared catalysts.

2.2. *UV-Vis spectroscopy*

UV-Vis spectroscopy was used for the speciation of Fe within each sample. Spectra were obtained on a Varian Cary 5000 spectrophotometer equipped with an external DRA-2500 in the range of 200 to 1500nm. Deconvolution of the UV-Vis spectra to Gaussian peaks was performed using *MagicPlot* software.

2.3. *BET characterization*

Nitrogen adsorption/desorption isotherms were performed at 77K using a gas absorption analyser (Tristar 3000) and pore size distributions and specific surface areas were calculated according to BJH and BET models respectively. Prior to N_2 adsorption, all samples were dried at 200°C under vacuum for 2 hours in order to remove any residual water.

2.4. *In-situ DRIFTS studies*

2.4.1. *NH₃ temperature programmed desorption (TPD)*

DRIFTS studies were used to investigate the formation and reaction of NH₃ on the surface of the catalyst. Pure BEA was used as a reference material in order to interpret the effect of the presence of iron species and any changes in activity due to ageing of the Fe/BEA zeolite. Spectra were recorded with a Biorad FTS6000 spectrometer at 1 cm⁻¹ resolution in a cell equipped with ZnSe windows. The samples were pretreated in a flow of Ar and O₂ at 500°C for 1 hour in order to remove any surface impurities and then cooled to 150°C under flowing Ar and a background spectrum was taken. The samples were then exposed to a flow of NH₃ and Ar for 30 minutes, followed by purging with Ar for a further 30 minutes. Temperature programmed desorption was then carried out in a flow of Ar from 150 to 500°C at 10°C/minute, flushed for a further 15 minutes and then cooled to room temperature. Spectra were obtained throughout the sequence with a time resolution of 5 per minute.

2.4.2. *NO temperature programmed desorption (TPD)*

The same protocol as for NH₃ TPD was used but in the presence of NO instead of NH₃. The machine was first purged with NO for 2 hours to remove any residual NH₃ as this would affect the adsorption of NO onto the samples.

2.4.3. *SCR reaction (NH₃, NO and 5% O₂)*

To analyse the SCR activity of the prepared catalysts they were saturated with NH₃ for 10 minutes at 250°C and balance Ar. Low temperature (250°C) was chosen so that the production of species during the reaction could be followed. Once saturated, samples were then exposed to a mixture of NO and O₂ in addition to NH₃ for a further 30 minutes. After this step, NH₃ was removed from the gas flow and the experiment was allowed to run in the presence of NO and O₂ for 30 minutes. The cell was then purged with Ar for 20 minutes. This method was chosen due to the extensive volume of groups who have done work to support the proposal that the SCR reaction occurs firstly by ammonia being strongly adsorbed to the catalyst surface, followed by interaction with NO via a gas phase or weakly adsorbed species. Due to time constraints, the catalysts aged at different temperatures (fresh, 700, 800 and 900°C) were focused upon since the samples aged at 700°C for different timescales showed very minor differences in the previous DRIFT experiments (NH₃ and NO TPD).

3. Results and Discussion

3.1. UV-vis Analysis

UV-vis spectroscopy was employed since it is a technique which is known to be capable of differentiating between the various iron structures which are present in the zeolite structure. Schwidder et al³⁵ proposed that the assignment of isolated Fe^{2+} and Fe^{3+} ions, oligomeric clusters inside pores and surface Fe_2O_3 particles, can be ascribed to bands present at <300, 335-385 and 460-550 nm respectively. This is in good accordance with the work of several other groups^{32,34,5} and so all spectra were deconvoluted within these specified ranges. The positioning of the bands was kept constant in all cases so that a fair comparison could be made. Positions were chosen according to the best fit of the obtained spectra and are summarized in table 1.

Table 1: Positioning of individual Fe species sub-bands within the UV-vis spectra

Fe species	Wavelength (nm)
Isolated Fe^{2+}	250
Isolated Fe^{3+}	280
Oligomeric Fe_xO_y clusters	365
Fe_2O_3 surface particles	460

A representative of these deconvoluted spectra can be seen in figure 3. It was chosen as it is the most intensely aged sample (48 hours at 900°C) and so, as a result of increased cluster and surface particle production, all sub-bands can be clearly observed. The areas of these sub-bands were used to calculate relative proportions of each iron species present in the sample.

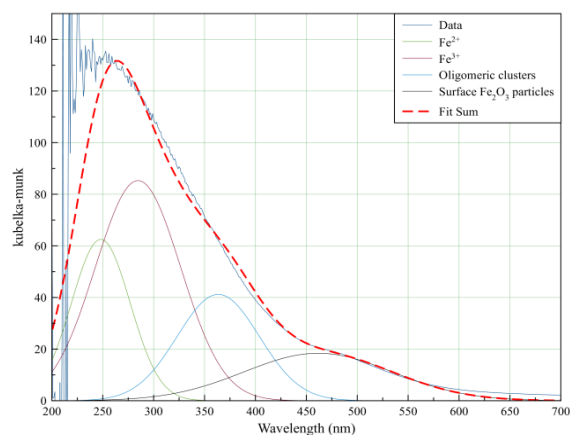


Figure 3: Deconvoluted UV-vis spectra of Fe/BEA aged for 48 hours at 900°C.

Table 2: Percentage of each Fe species present within the respective catalyst samples as a result of the deconvolution of UV-vis spectra

Fe Species	Iron content of catalyst sample (%)						
	Fresh sample	6h aged 700°C	12h aged 700°C	24h aged 700°C	48h aged 700°C	48h aged 800°C	48h aged 900°C
Fe ²⁺	32.85	24.97	24.52	22.48	22.57	22.37	21.52
Fe ³⁺	53.60	60.65	61.63	64.71	65.16	47.65	42.67
Oligomeric Fe _x O _y clusters	9.57	10.92	12.14	10.38	10.32	14.95	19.80
Fe ₂ O ₃ particles	3.98	3.46	1.71	2.42	1.95	15.03	16.00

The deconvoluted spectra of all remaining samples can be found in appendix a.

A summary of the relative proportion of the iron species present in each sample can be seen in Table 2. It shows that a slight decrease in the percentage of Fe²⁺ and Fe₂O₃ coupled with a subsequent increase in the proportion of Fe³⁺ and oligonuclear clusters, is observed upon increasing time of exposure to thermal treatment at 700°C. However, there is very little difference between the iron content of the samples aged at this temperature. This may be due to the fact that there is no water present in the ageing process and so the migration of isolated iron ions out of ion exchange sites and the possibility of zeolite dissolution and dealumination is limited. Also, as the ageing process was run at 700°C, we would not expect significant degradation of the zeolite structure as this has been reported to take place at around 850°C and so we would not expect for the iron sites to be affected significantly⁵.

However, upon ageing the catalyst at higher temperatures (800 and 900°C) it can be seen that, the percentage of isolated Fe²⁺ ions present remains relatively unaltered, possible suggesting that these remaining ions are quite stable in their exchange positions. There is also a much higher percentage of iron oxide clusters and particles now present as a result of the conversion of Fe³⁺ ions within the structure. This may be explained by a change in the structure of the zeolite itself and thus further characterization (BET) is necessary in order to confirm whether or not this is the case. It is thought that these larger particles and clusters are inactive in the SCR reaction and so comparison of these higher aged samples may help to determine whether their production is indeed responsible for the deactivation of the catalyst.

3.2. BET characterization

Table 3 shows that, as the catalyst becomes aged for extended periods of time and/or under higher temperature conditions, the surface area of the catalyst decreases whilst the average pore width increases.

The difference is initially very small when the catalyst is aged at 700°C for differing timescales. However, the difference in surface area between the samples aged at differing temperature for 48 hours is an important effect. It shows that the thermal treatment at high temperatures is likely to be having a destructive effect on the zeolite framework itself, allowing for greater migration of iron and may be the reason that clusters are able to form in the absence of water.

In previous studies, these two steps have been linked together since framework aluminium is known to act as an exchange site for the cationic iron species; upon dealumination, the iron ions occupying exchange sites are replaced by cationic aluminium species allowing for increased migration and therefore clustering of the iron species⁴². However, these studies were conducted in the presence of water so it is interesting to see that the same trend has been observed when water was absent from the ageing process. Since the samples were aged in the presence of air, it may also be possible that the small amount of water which is available in the air is enough to allow the dealumination of the zeolite framework to take place.

Table 3: BET characterization of Fe/BEA aged under differing temperatures and timescales

	Fresh sample	12 hour aged 700°C	24 hour aged 700°C	48 hour aged 700°C	48 hour aged 800°C	48 hour aged 900°C
BET surface area (m ² /g)	627.0	555.1	552.1	507.0	293.7	10.5
Average pore width (Å)	22.9	23.1	23.2	23.7	29.1	127.6

3.3. DRIFTS characterization

All DRIFTS spectra presented in this work are referred to as ‘difference spectra’. This means that a background spectra was taken of the pretreated catalyst before exposure to any gas mixtures. Therefore, what we observe during each reaction is the change in active sites of the catalyst as a result of adsorption and desorption of gaseous species on their surface.

3.3.1. NH_3 TPD

Ammonia was chosen as a probe molecule, not only because of its role in the standard SCR reaction, but also because it is capable of providing an insight into the availability and adsorption of ammonium onto Brønsted acid sites as well as Lewis acid sites²³. This information is sensitive to the zeolite structure and so should show any changes in structure which occur as a result of the ageing process.

Figure 4 shows the DRIFT spectra of pure BEA zeolite undergoing the NH_3 TPD reaction obtained at significant times of exposure and temperature. The broad features present in the region of 2400 to 3300 cm^{-1} make specific assignments of peaks ambiguous as many conflicting propositions exist within the literature. However, some agreements have been found and so the peak at 2965 cm^{-1} has been selected to represent NH_4^+ ions bound by 2 hydrogen atoms to AlO_4 tetrahedra^{23,22}. The peaks observed at 3372 and 3261 cm^{-1} were ascribed to the asymmetric and symmetric NH stretches of ammonia which is formed on

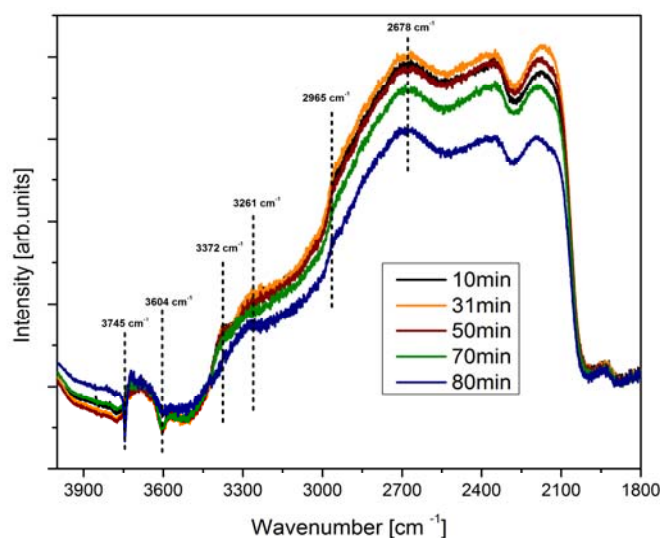


Figure 4: DRIFT spectra following the reaction of NH_3 TPD on pure BEA

Brønsted acid sites respectively^{23,7} and the broad peak observed at $\sim 2678\text{ cm}^{-1}$ was due to the presence of weakly bound ammonia on the zeolite^{28,7}. The negative peaks observed at 3745 cm^{-1} and 3604 cm^{-1} were present due to the adsorption of ammonia, some of which is hydrogen bonded to terminal silanol and SiOHAl groups of the zeolite respectively^{23,28,34}.

Since there is a large contribution of noise present in the spectra below 1800 cm^{-1} , the effect which the presence of isolated Fe species has in the presence of NH_3 could not be observed. This is because the bands produced as a result of the high affinity for NH_3 adsorption on the zeolite had such a large contribution to the spectra.

It should be noted that there is significantly less ammonia being retained during the TPD process on those catalysts which are aged at higher temperatures compared to the fresh iron-containing sample and the pure BEA zeolite (see appendix b). This can be observed by following the reaction over time and comparing the difference in intensity of each spectra in the region which ammonia adsorption and desorption on the zeolite support is observed (2800 to 3400 cm^{-1}).

In all cases an initial increase in intensity from the start of the provision of ammonia (10 minutes) until full saturation is reached (31 minutes). After this point, when ammonia is subsequently absent from the gas feed and the system is being purged with argon, a small decrease in the intensity of the signal is observed due to the removal of weakly physisorbed species. After 50 minutes the temperature is rapidly increased, resulting in a much greater loss of adsorbed NH_3 and NH_4^+ . This can be observed by the increasing difference in intensity of the spectra obtained between 50 and 70 minutes as well as the difference between the spectra at 70 and 80 minutes. When the catalyst is subjected to a more intense ageing process, the removal of these species from the surface occurs at a much faster rate, suggesting that the ammonia is less strongly adsorbed to the zeolite structure. Thus, what we may be observing is small differences in the zeolite framework itself as a result of thermal treatment.

It can also be seen from figures 5 and 6 that, as the Fe/BEA is exposed to thermal ageing for increased lengths of time and/or elevated temperature, the availability of Brønsted acid sites available for ammonia adsorption decreases. This can be concluded due to the reduced intensities of the spectra observed around $\sim 2700\text{ cm}^{-1}$ relative to the peaks produced as a result symmetric and asymmetric stretches of NH present between 3280 and 3360 cm^{-1} . Interestingly, it could also be seen that the catalyst which was aged at 900°C showed very limited adsorption of gaseous species. This is thought to be due to the destruction of the

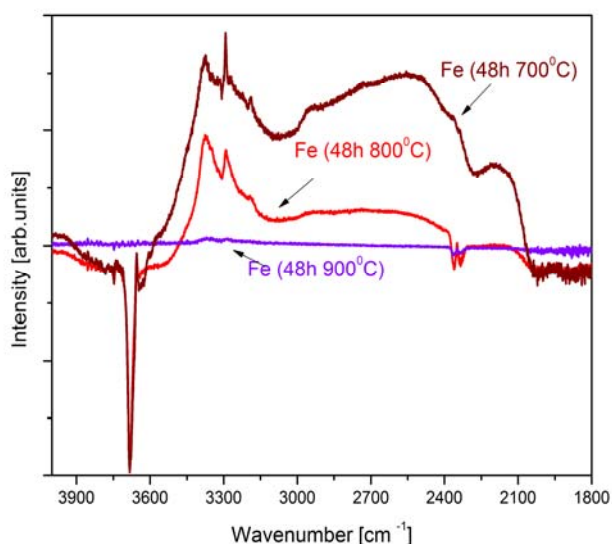


Figure 5: DRIFT spectra of NH_3 TPD of Fe/BEA aged for 48 hours at varying temperatures

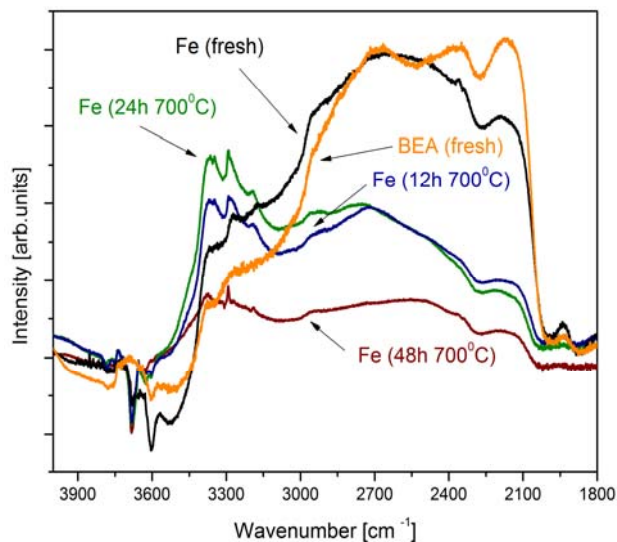


Figure 6: DRIFT spectra of NH_3 TPD of Fe/BEA samples aged at 700°C for varying timescales

zeolite support as shown by the BET analysis but further analysis must be carried out before we can conclude this with confidence.

This loss of ammonium adsorption capacity is a very interesting and relevant trend since, as previously discussed, Brønsted acidity is considered to be an important factor in the SCR reaction since it is thought to take place via an Eley-Rideal mechanism, requiring ammonium ions to be surface bound in order to react with nearby weakly adsorbed nitrous oxides or gas molecules.

As the ageing process becomes more aggressive (particularly under high temperature conditions), it can also be seen that the contribution of the peaks which represent the binding of NH_4^+ to alumina ($\sim 2965\text{ cm}^{-1}$) and ammonia to SiOHAl ($\sim 3604\text{ cm}^{-1}$) become less distinct. Again this suggests a change in the structure of the zeolite framework itself, consistent with the proposed theory of deactivation as a result of dealumination of the zeolite.

The presence of iron occupying the exchange sites of the BEA zeolite could also be confirmed upon comparison of the ammonia adsorption spectra of the pure BEA control sample (figure 3) and the remaining iron-containing samples, observed in figure 7. This was due to the appearance of a large negative peak at $\sim 3682\text{ cm}^{-1}$ which represents $\text{Fe}(\text{OH})_2$ Brønsted acid groups and is consistent with the literature³⁴. Spectra were aligned using the minima at 3655 cm^{-1} as a reference point so that a direct comparison could be made regarding the intensities

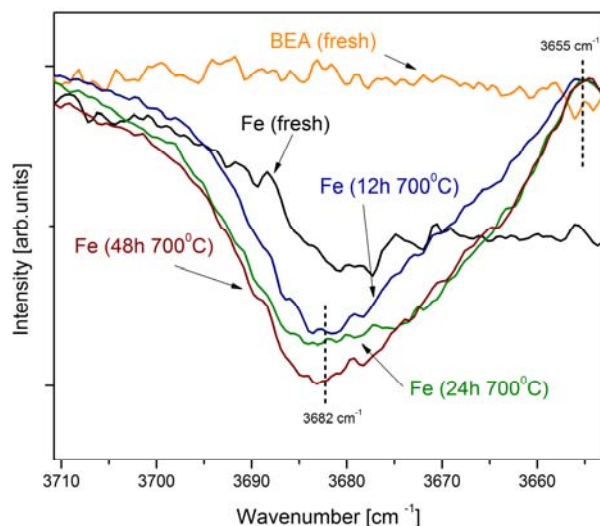


Figure 7: DRIFT spectra of NH_3 adsorption on iron sites of BEA samples

of these $\text{Fe}(\text{OH})_2$ peaks. As the fresh sample produced a rather broad signal at this range it was placed in accordance with the BEA spectra. It can be seen that, as the catalyst is aged for longer periods of time, the contribution of these groups to the NH_3 adsorption increases, suggesting that these sites were becoming increasingly blocked. This may be a result of the production of larger particles although this cannot be deduced conclusively from the NH_3 TPD results alone.

It is also of interest to note that the intensity of this peak is not largely affected during the cleaning of the surface, as can be seen in figure 8. This is much different than when comparing to the effect which the cleaning program has in the 2800 to 3400 cm^{-1} range previously discussed, implying that ammonia is more stable when adsorbed to $\text{Fe}(\text{OH})_2$ Brønsted sites than when adsorbed onto the Brønsted acid sites of the zeolite structure itself.

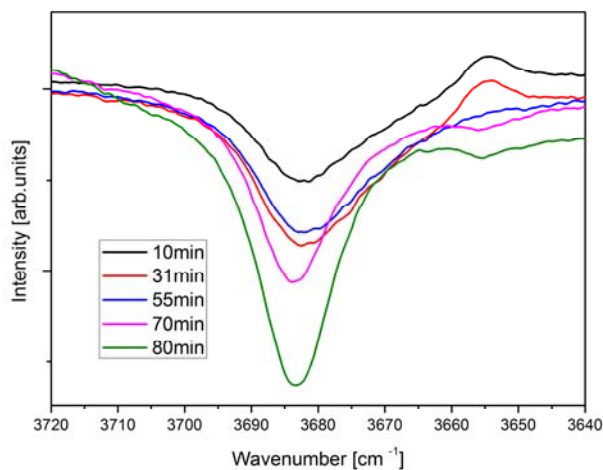


Figure 8: DRIFTS spectra of $\text{Fe}(\text{OH})_2$ peak at different stages during NH_3 TPD reaction

3.3.2. NO TPD

NO was chosen to analyse the adsorption properties of the catalyst, not only because of its role in the SCR reaction, but also because it is a good probe molecule with a high affinity for iron species, capable of providing insight into their location, form and behaviour⁴³. It can be seen from figure 9 that there is minimal contribution by the zeolite support in the presence of NO in the main region of interest.

The peaks present at $\sim 2130\text{ cm}^{-1}$ have been reported to be a result of the adsorption of NO^+ onto both isolated Fe^{3+} species²⁸ and also Brønsted acid sites of the zeolite support⁴³. When comparing the spectra obtained by the pure BEA and the unaged Fe/BEA in figure 9, it could be claimed that both suggestions are substantiated in this study. The addition of Fe to the zeolite increased the intensity of the signal slightly indicating an initial increase in the volume of sites for NO adsorption to take place at. The relative intensity of this peak reduces as the catalyst becomes more aged, indicating a change in the zeolite support, a decrease in volume of isolated Fe^{3+} species or in fact both. Both of these conclusions have been supported by the previous analyses. The change in structure of the zeolite support is in good accordance with the results obtained during the NH_3 TPD and BET experiments, showing that the Brønsted acidity of the catalysts is greatly affected by thermal degradation. The reduction in Fe^{3+} species was confirmed by UV-vis analysis and is as expected for thermally treated samples due to clustering.

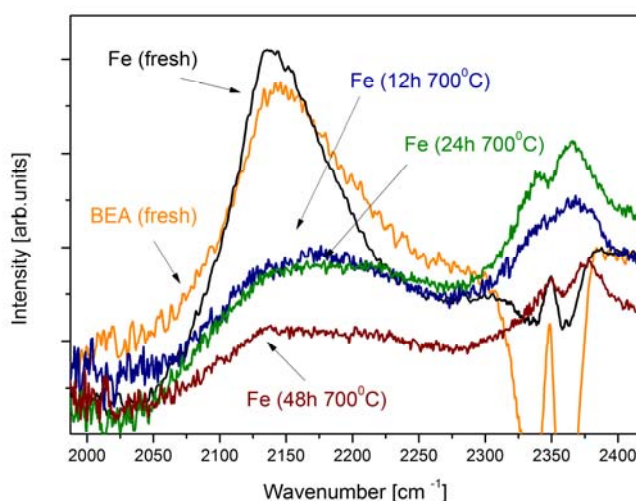


Figure 5: DRIFT spectra of NO^+ adsorption on BEA catalysts

For NO adsorption, it has been found that adsorption onto differing Fe species can be distinguished between and occurs within the range of ~ 1600 to 1870 cm^{-1} . The peak observed at $\sim 1870\text{ cm}^{-1}$ is representative of NO adsorbed onto both isolated Fe^{2+} in ion-exchange positions and $\text{Fe}_x^{2+}\text{O}_y$ oligonuclear species present in zeolite cavities^{28,43,33} whilst the peak present at $\sim 1630\text{ cm}^{-1}$ is due to the adsorption of NO_2 onto larger $\text{Fe}_x^{3+}\text{O}_y$ species^{34,22,7}, although it should be noted that the bending mode of water can also be expected at this wavenumber^{23,7}. The assignment of this peak to oxo- Fe^{3+} species such as large Fe_2O_3 particles makes sense since the gas feed consisted of NO only and the conversion to NO_2 has been suggested to take place by the presence of releasable oxygen atoms on Fe^{3+} species which are subsequently transported to the NO molecule³⁴.

Figures 10 and 11 show that as the catalysts are aged for greater lengths of time and/or more intense temperature, not only is there an increased production of these clustered species, the ratio of the Fe^{3+} species to Fe^{2+} also increases greatly. This indicates a greater proportion of large clusters and possibly even surface particles being formed as the ageing process progresses. The presence of these large clusters may suggest that the catalyst is becoming decreasingly active but cannot be said conclusively since there is some discrepancy among the literature regarding the role of these species in the SCR reaction. As a further test, it may be interesting to carry out some activity testing on these samples to view the effect that the ageing is having upon conversion properties, especially as the adsorption of NO_2 is considered a prerequisite of the occurrence of the SCR reaction.

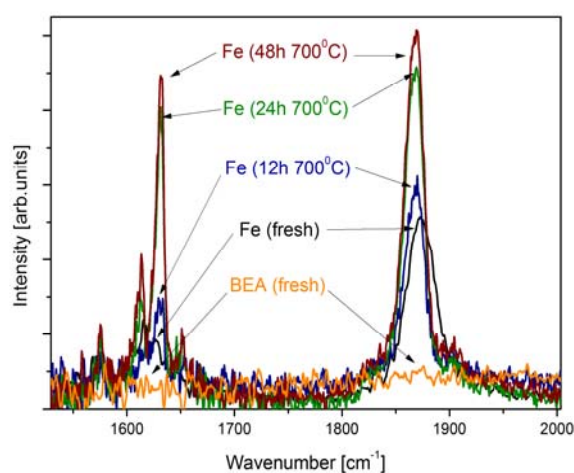


Figure 10: DRIFT spectra of NO adsorption on Fe/BEA samples aged at 700°C for varying timescales

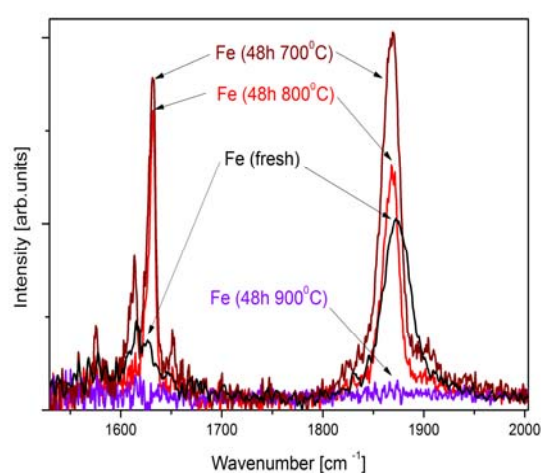


Figure 11: DRIFT spectra of NO adsorption on Fe/BEA samples aged for 48 hours for varying temperatures

It can also be seen that as the catalysts become more aged, there is a greater presence of nitrate (NO_3^-) adsorption on Fe species. This is indicated by the presence of the peak at $\sim 1610 \text{ cm}^{-1}$ increasing in intensity with age²².

As with the NH_3 TPD tests, once the catalyst is aged at 900°C the adsorption of NO is no longer observed, implying a change in the local structure of the zeolite support (see figure 11). However, this does not exclusively mean that this catalyst is no longer SCR active as Peden *et al*⁴⁴ have found that destroying the zeolite support may, in some cases, actually enhance activity. They proposed that, upon dealumination of Cu/BEA zeolite, the copper species strongly interacted with the aluminium and that this phase was responsible for an increase in the SCR activity of the catalyst. It would therefore be of interest to carry out further activity tests on this material to determine whether it is still effective in the selective reduction of NO_x .

3.3.3. SCR Reaction

Figure 12 compares the DRIFT spectra obtained during the SCR reaction on the fresh catalyst and those aged under different temperature conditions (700 , 800 and 900°C). As before, the catalyst aged at 900°C showed no adsorption and so the following discussion does not include this particular sample.

The spectra obtained after 10 minutes of reaction correspond to adsorption of NH_3 onto the catalyst samples. As would be expected, these spectra showed the same features as with the TPD experiments and confirmed the adsorption of ammonia onto Brønsted acid sites. This could be concluded due to the negative peaks observed at $\sim 3680 \text{ cm}^{-1}$ which corresponds to the blocking of the active sites by the ammonia and also the broad positive peak around 2700 cm^{-1} which is representative of the NH stretching range of ammonium weakly bound to the zeolite framework. This experiment correlated with the previous conclusions reached from the NH_3 TPD experiment because it shows the increased ammonium adsorption capacity of the fresh sample compared to those which are aged.

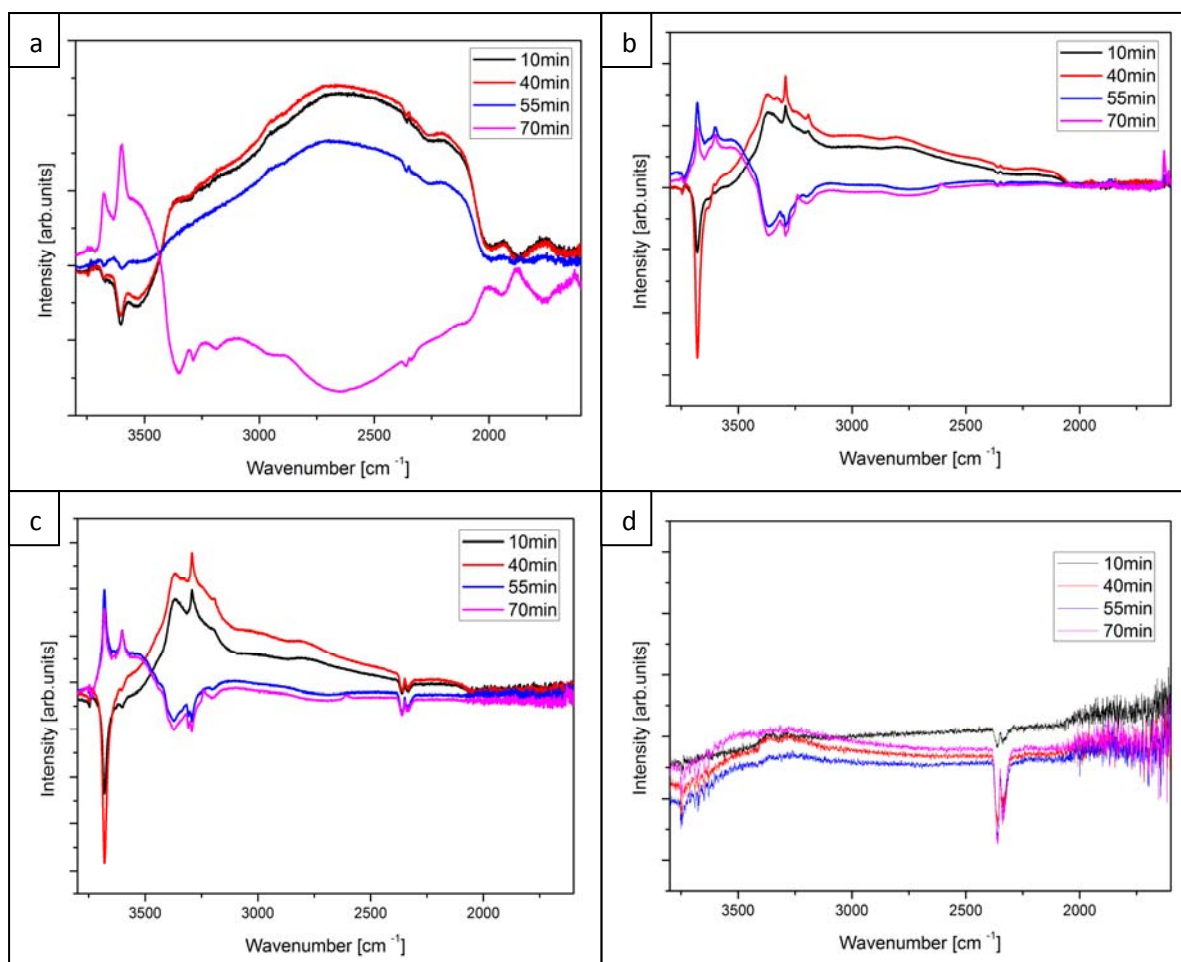


Figure 12: DRIFT spectra following the SCR reaction on (a) Fresh Fe/BEA, (b) Fe/BEA aged at 700°C for 48 hours, (c) Fe/BEA aged at 800°C for 48 hours and (d) Fe/BEA aged at 900°C for 48 hours

After 40 minutes, when NO and O₂ were introduced in the gas flow as well as NH₃, the aged samples showed a further decrease in intensity of the negative Fe(OH)₂ peak whereas the fresh sample showed a very subtle increase in intensity. This implied that the aged samples were not fully saturated in the first step and so more ammonia was being adsorbed onto the Brønsted acid sites whereas the adsorbed ammonia was rapidly consumed by NO in the case of the fresh catalyst.

Once NH₃ is removed from the feed, the negative peak at ~3680 cm⁻¹ becomes increasingly positive with time (55 and 70 minute spectra) in all samples, suggesting the consumption of adsorbed ammonia and the unblocking of the active sites. This confirms that in all cases the Brønsted acid sites are participating in the SCR reaction. The removal of weakly adsorbed ammonia could also be seen by the decrease in intensity of the peaks in the 3200 to 3500 cm⁻¹

region which represents the symmetric and asymmetric NH stretching of ammonia which is bound to Brønsted acid sites of the zeolite.

When comparing the aged samples to the fresh, it can be seen that the ammonia is removed from the surface much quicker for those samples which are aged. This could be said because when spectra were obtained at 55 minutes, the fresh catalyst still showed a negative peak at $\sim 3680\text{ cm}^{-1}$ and broad positive peaks in the NH stretching region whereas the aged catalysts no longer shared these features. In fact the opposite was observed (a positive peak at $\sim 3680\text{ cm}^{-1}$ and negative bands in the NH stretching region) indicating that the catalyst surface had already been cleaned of any adsorbed NH_3 species. This may be due to the reduced ammonia adsorption capacity as previously discussed and so the adsorbed ammonia is being consumed much more quickly.

Although this experiment showed that all samples were SCR active, a suggestion for further work would be to carry out activity tests on these samples so that direct comparisons of their effectiveness for NO_x reduction can be made.

4. Conclusions

- Increasing the temperature and time of thermal treatment of Fe/BEA results in increased production of iron clusters and a subsequent loss of isolated Fe^{2+} ions which are considered to be the most active species in the SCR reaction. This is most likely to be due to migration of the ions through the structure.
- As the catalysts are subjected to higher temperatures, there is a decrease in surface area observed, due to the eventual collapse of the zeolite framework. This in turn leads to a reduction in the Brønsted acid sites available in the sample and so the ammonia adsorption capacity is reduced.
- As the Fe/BEA was subjected to more aggressive ageing conditions, the NO oxidation increased, most likely as a result of the increased proportion of oxo-Fe species available to donate releasable oxygen atoms.
- A recommendation for future work would be to carry out activity tests on these catalysts to see what the combined effect of reduced ammonia adsorption capacity and increased NO oxidation has on their SCR activity. These would, not only be likely to give more information on the SCR activity of these catalysts, but, by comparing the results to the dominant species present in each sample, may also help to determine the roles which the iron species are responsible for.

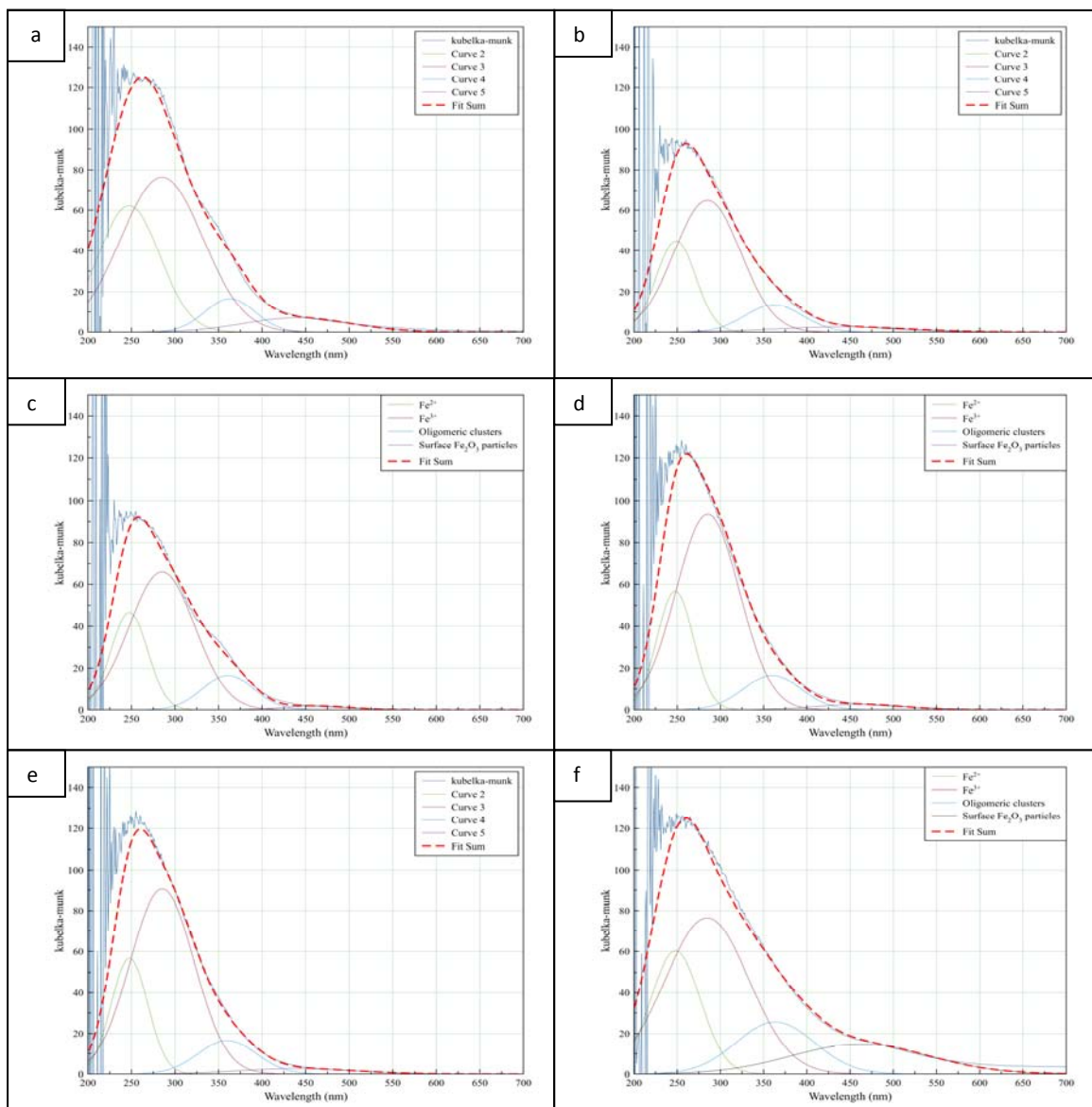
5. References

1. K. Rahkamaa-Tolonen, T. Maunula, M. Lomma, M. Huuhtanen, and R. L. Keiski, *Catal. Today*, 2005, **100**, 217-222.
2. C. He, Y. Wang, Y. Cheng, C. K. Lambert, and R. T. Yang, *Appl. Catal. A: Gen.*, 2009, **368**, 121-126.
3. S. Brandenberger, O. Kröcher, A. Tissler, and R. Althoff, *Catal. Rev.*, 2008, **50**, 492-531.
4. M. L. M. de Oliveira, C. M. Silva, R. Moreno-Tost, T. L. Farias, A. Jiménez-López, and E. Rodríguez-Castellón, *Appl. Catal. A: Gen.*, 2009, **366**, 13-21.
5. L. Ma, J. Li, H. Arandiyán, W. Shi, C. Liu, and L. Fu, *Catal. Today*, 2011, **184**, 145-152.
6. *www.commercialmotors.com*, accessed 04/05/2012.
7. M. Wallin, C. J. Karlsson, A. Palmqvist, and M. Skoglundh, *Top. Catal*, 2004, **30**, 107-113.
8. A. Grossale, I. Nova, and E. Tronconi, *Catal. Today*, 2008, **136**, 18-27.
9. M. Wallin, C. J. Karlsson, M. Skoglundh, and A. Palmqvist, *J. Catal*, 2003, **218**, 354-364.
10. M. Eichelbaum, A. B. Siemer, R. J. Farrauto, and M. J. Castaldi, *Appl. Catal. B: Environ.*, 2010, **97**, 98-107.
11. J. A. Anderson and M. F. Garcia, *Supported Metals in Catalysis*, 2005.
12. C. H. Bartholomew, *Appl. Catal. A: Gen.*, 2001, **212**, 17-60.
13. *www.dieselnet.com*, accessed 21/11/2011.
14. J. Li, H. Chang, L. Ma, J. Hao, and R. T. Yang, *Catal. Today*, 2011, **175**, 147-156.
15. P. Balle, B. Geiger, D. Klukowski, M. Pignatelli, S. Wohnrau, M. Menzel, I. Zirkwa, G. Brunklaus, and S. Kureti, *Appl. Catal. B: Environ.*, 2009, **91**, 587-595.
16. M. Koebel, M. Elsener, and M. Kleemann, *Science*, 2000, **59**, 335-345.
17. Z. Li, L. T. Shen, W. Huang, and K. C. Xie, *J. Environ. Sci.*, 2007, **19**, 1516-9.
18. A. Lindholm, H. Sjövall, and L. Olsson, *Appl. Catal. B: Environ.*, 2010, **98**, 112-121.

19. D. Chatterjee, P. Kočí, V. Schmeißer, M. Marek, M. Weibel, and B. Krutzsch, *Catal. Today*, 2010, **151**, 395-409.
20. R. Bonzi, L. Lietti, L. Castoldi, and P. Forzatti, *Catal. Today*, 2010, **151**, 376-385.
21. O. Krocher, *Stud. Surf. Sci. Catal.*, 2007, **171**, 261-289.
22. M. Devadas, O. Krocher, M. Elsener, A. Wokaun, N. Soger, M. Pfeifer, Y. Demel, and L. Mussmann, *Appl. Catal. B: Environ.*, 2006, **67**, 187-196.
23. Z. Liu, P. J. Millington, J. E. Bailie, R. R. Rajaram, and J. A. Anderson, *Micropor. Mesopore. Mat.*, 2007, **104**, 159-170.
24. G. Zhou, B. Zhong, W. Wang, X. Guan, and B. Huang, *Catal. Today*, 2011, **175**, 157-163.
25. H. S. Park, G. Seo, Y. Yoo, and H. Han, *Korean J. Chem. Eng.*, 2010, **27**, 1738-1743.
26. J. Y. Luo, X. Hou, P. Wijayakoon, S. J. Schmieg, W. Li, and W. S. Epling, *Appl. Catal. B: Environ.*, 2011, **102**, 110-119.
27. www.personal.utulsa.edu, accessed 04/05/12.
28. D. Klukowski, P. Balle, B. Geiger, S. Wagloehner, S. Kureti, B. Kimmerle, A. Baiker, and J. Grunwaldt, *Appl. Catal. B: Environ.*, 2009, **93**, 185-193.
29. S. Brandenberger, O. Kröcher, M. Casapu, A. Tissler, and R. Althoff, *Appl. Catal. B: Environ.*, 2011, **101**, 649-659.
30. T. J. Toops, K. Nguyen, A. L. Foster, B. G. Bunting, N. A. Ottinger, J. A. Pihl, E. W. Hagaman, and J. Jiao, *Catal. Today*, 2010, **151**, 257-265.
31. B. Dedecek, J. Capek, L. Sazama, P. Sobalik, Z. Wichterlova, *Appl. Catal. A: Gen.*, 2011, **391**, 244-253.
32. M. Santhoshkumar, M. Schwidder, W. Grunert, U. Bentrup, and A. Bruckner, *J. Catal.*, 2006, **239**, 173-186.
33. M. Kim, K. W. Lee, J. Park, C. Shin, J. Lee, and G. Seo, *Zeolites*, 2010, **27**, 76-82.
34. M. Iwasaki, K. Yamazaki, K. Banno, and H. Shinjoh, *J. Catal.*, 2008, **260**, 205-216.
35. M. Schwidder, M. S. Kumar, K. Klementiev, M. Martina, A. Brückner, and W. Grünert, *J. Catal.*, 2005, **231**, 314-330.
36. A. Tissler, R. Althoff, S. Brandenberger, and O. Kröcher, *Appl. Catal. B: Environ.*, 2010, **95**, 348-357.
37. M. Mihaylov, E. Ivanova, K. Chakarova, P. Novachka, and K. Hadjiivanov, *Appl. Catal. A: Gen.*, 2011, **391**, 3-10.

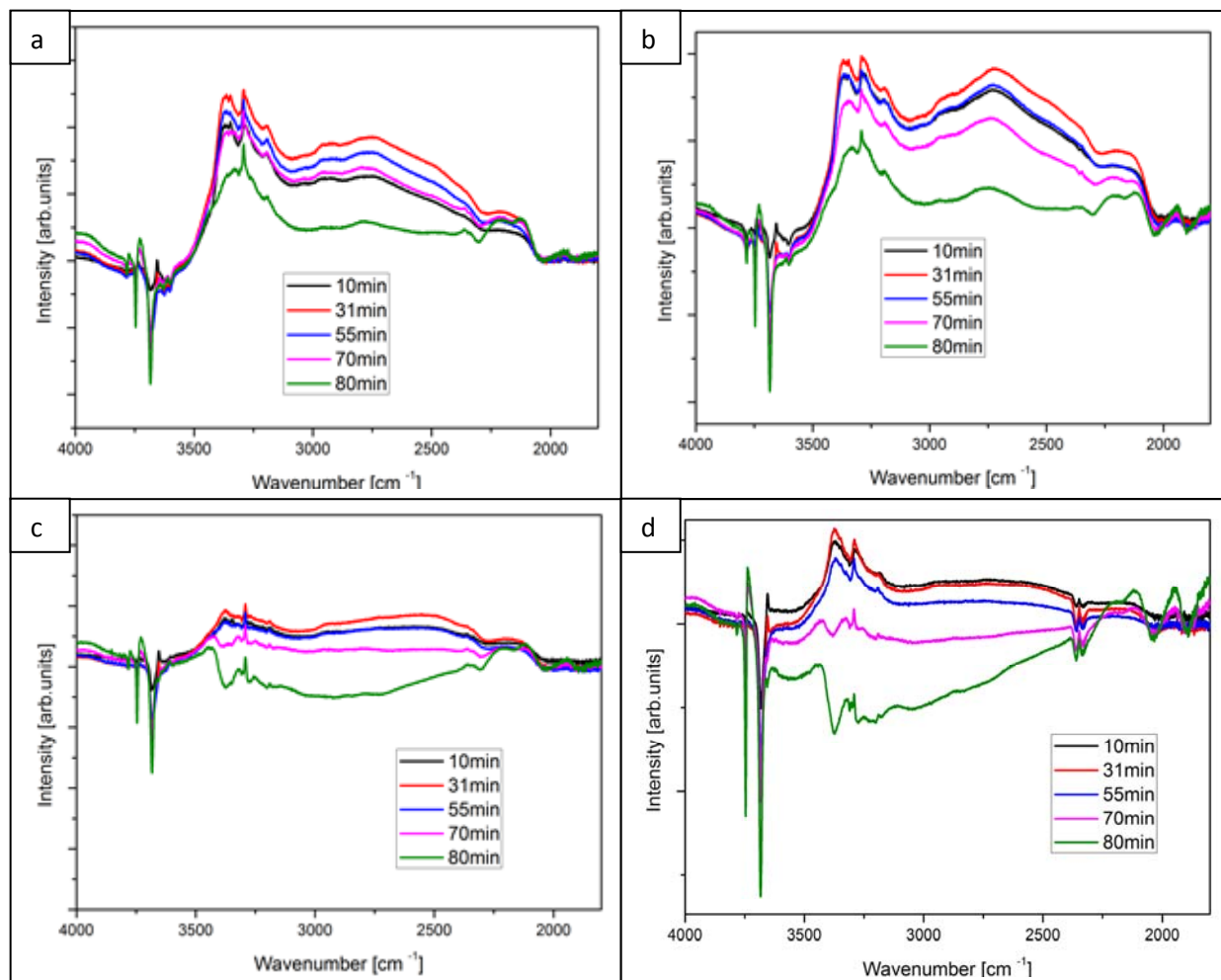
38. A. Beers, *J. Catal*, 2003, **218**, 239-248.
39. R. Long and R. Yang, *J. Catal*, 2002, **207**, 224-231.
40. P. Kern, M. Klimeczak, T. Heinzelmann, M. Lucas, and P. Claus, *Appl. Catal. B: Environ.*, 2010, **95**, 48-56.
41. M. A. Centeno, I. Carrizosa, and J. A. Odriozola, *Appl. Catal. B: Environ.*, 1998, **19**, 67-73.
42. J. Pieterse, G. D. Pirngruber, J. Van-Bokhoven, and S. Booneveld, *Appl. Catal. B: Environ.*, 2007, **71**, 16-22.
43. G. Mul, M. W. Zandbergen, F. Kapteijn, J. A. Moulijn, and J. Perez-Ramirez, *Catal. Letters*, 2004, **93**, 113-120.
44. C. H. F. Peden, J. Hun, S. D. Burton, R. G. Tonkyn, D. Heui, J. Lee, H. Jen, G. Cavataio, Y. Cheng, and C. K. Lambert, *Catal. Today*, 2012, **184**, 245-251.

Appendix a.



Appendix a: Deconvolution of UV-vis spectra of (a) Fresh Fe/BEA, (b) 700°C 6 h aged Fe/BEA, (c) 700°C 12 h aged Fe/BEA, (d) 700°C 24 h aged Fe/BEA, (e) 700°C 48 h aged Fe/BEA and (f) 800°C 48 h aged Fe/BEA

Appendix b.



Appendix b: DRIFT spectra following the reaction of NH₃ TPD on (a) Fe/BEA aged at 700°C for 12h (b) Fe/BEA aged at 700°C for 24h, (c) Fe/BEA aged at 700°C for 48h, and (d) Fe/BEA aged at 800°C for 48h,